Published for SISSA by Springer

Received: *December 12, 2014*
Revised: *June 18, 2015*
Accepted: *August 3, 2015*
Published: *August 27, 2015*

Quantum black holes and their lepton signatures at the LHC with CalCHEP

Alexander Belyaev[a,b] **and Xavier Calmet**[c]

[a] *School of Physics and Astronomy, University of Southampton, Highfield, Southampton SO17 1BJ, U.K.*
[b] *Particle Physics Department, Rutherford Appleton Laboratory, Chilton, Didcot, Oxon OX11 0QX, U.K.*
[c] *Physics and Astronomy, University of Sussex, Falmer, Brighton, BN1 9QH, U.K.*

E-mail: a.belyaev@soton.ac.uk, x.calmet@sussex.ac.uk

Abstract: We discuss a field theoretical framework to describe the interactions of non-thermal quantum black holes (QBHs) with particles of the Standard Model. We propose a non-local Lagrangian to describe the production of these QBHs which is designed to reproduce the geometrical cross section πr_s^2 for black hole production where r_s is the Schwarzschild radius. This model is implemented into CalcHEP package and is publicly available at the High Energy Model Database (HEPMDB) for simulation of QBH events at the LHC and future colliders. We present the first phenomenological application of the QBH@HEPMDB model with spin-0 neutral QBH giving rise the e^+e^- and $e\mu$ signatures at the LHC@8TeV and LHC@13TeV and produce the respective projections for the LHC in terms of limits on the reduced Planck mass, $\overline{M}_{PL}$ and the number of the extra-dimensions n.

Keywords: Phenomenological Models, Monte Carlo Simulations

ArXiv ePrint: 1412.2661

doi:10.1007/JHEP08(2015)139

JHEP08(2015)139

Contents

1 Introduction and model setup

Realising that the Planck mass (M_{PL}) may not be around 10^{19} GeV but that it is a model dependent quantity which could even be as low as a few TeVs has had a considerable impact in particle physics [1–6]. One of the most amazing signatures of these models would be the creation of small black holes at colliders [7–11] or in the scattering of cosmic rays [12–19] in the upper atmosphere of our planet. While it is now well appreciated that semi-classical black holes cannot be produced at the LHC because this collider is not energetic enough even if M_{PL} is at a few TeVs [20], the possibility remains to produce non-thermal quantum black holes (QBHs) [11].

Let us first define clearly what we mean by QBHs. We define QBHs as black holes with masses of the order of M_{PL}. These black holes are thus fully quantum gravitational objects. They will thus be non-thermal objects and their decomposition is thus not expected to be well described by Hawking radiation. One way to think of QBHs is of an extrapolation into the full quantum regime of semi-classical black holes, which have been extensively studied [7–10, 12–15, 19, 21–25]. Semi-classical black holes have masses between 5 to 20 times larger than the Planck scale. They are thus thermal objects because of the ratio between their masses and M_{PL}, and will they will therefore decay via Hawking radiation. Their physics is thus rather different from that of QBHs.

If black holes are produced at the LHC, they will be produced very near the kinematical threshold which is defined by M_{PL}. This happens because the production of higher mass black holes, as we will demonstrate below, will be strongly suppressed by the parton density distributions (PDFs) which are steeply falling with masses. Given the center of mass energy of the LHC, it is very unlikely to produce semi-classical black holes even if M_{PL} is in the few TeVs region. On the other hand, QBHs could be produced copiously since their masses are close to this kinematical threshold and thus M_{PL}.

Because QBHs are fully quantum gravitational objects, it is difficult to derive their production cross section from first principles. The only possible approach is to extrapolate their production cross section from that obtained in the semi-classical limit. Besides this they will not decay via Hawking radiation since they are non-thermal objects. Using the semi-classical expression for the decay multiplicity of a semi-classical black hole and extrapolating to the limit where the ratio of its mass to M_{PL} goes to one, one finds that the multiplicity for a QBH tends towards 2. Obviously, this approximation is not a valid one, but this is the best that can be done given our current understanding of quantum gravitational effects. This is what one would expect from a non-thermal object which should not decay into many particles. Therefore we assume that QBHs will decay into just a few particles resembling strong gravitational re-scattering.

It is thus tempting to treat QBHs as particles with a mass and carrying the quantum numbers of the particles which created them. In a proton collider, there will be quarks and gluons. The aim of this paper is to extend the work presented in [26, 27] where a field theoretical model to describe the interactions of non-thermal QBHs with the particles of the standard model was proposed. This framework assumes that QBHs can be treated as quantum fields, i.e. they are classified according to representations of the Lorentz group. Furthermore, they are classified according to their transformations under the gauge groups of the standard model. This fixes their interactions with matter.

In a proton-proton collider, QBHs would be produced from the collisions of quarks and gluons if the Planck scale is low enough. We are thus particularly interested in the QBHs carrying QCD and QED quantum numbers and with spins 0,1/2 and 1 since these should be the lowest lying states. Generically speaking, QBHs form representations of $\mathrm{SU}(3)_c$ and carry a QED charge. The process of two partons p_i, p_j forming a quantum black hole in the c representation of $\mathrm{SU}(3)_c$ and charge q as: $p_i + p_j \to \mathrm{QBH}_c^q$ is considered in [11]. The following different transitions are possible at a proton collider:

a) $\mathbf{3} \times \overline{\mathbf{3}} = \mathbf{8} + \mathbf{1}$

b) $\mathbf{3} \times \mathbf{3} = \mathbf{6} + \overline{\mathbf{3}}$

c) $\mathbf{3} \times \mathbf{8} = \mathbf{3} + \overline{\mathbf{6}} + \mathbf{15}$

d) $\mathbf{8} \times \mathbf{8} = \mathbf{1}_S + \mathbf{8}_S + \mathbf{8}_A + \mathbf{10} + \overline{\mathbf{10}}_A + \mathbf{27}_S$

Most of the time the black holes which are created carry a $\mathrm{SU}(3)_c$ charge and come in different representations of $\mathrm{SU}(3)_c$ as well as QED charges. This allows the prediction of how they will be produced or decay. The aim of this work is to propose a framework to describe these interactions.

As emphasized above, we will extrapolate the production cross section for QBHs from the semi-classical one which is determined by the Schwarzschild radius, i.e. we assume that the cross section for QBHs is given by the geometrical formula (see e.g. [21–24])

$$\sigma = \pi r_s^2 \tag{1.1}$$

where r_s is the four-dimensional Schwarzschild radius

$$r_s(s, \overline{M}_{PL}) = \frac{\sqrt{s}}{4\pi \overline{M}_{PL}^2}, \tag{1.2}$$

where s is the invariant mass of the colliding particles, which upon exceeding the reduced Planck mass, $\overline{M}_{PL}$ creates the respective QBH with the continuous mass equal to $\sqrt{s}$. So, in terms of s and $\overline{M}_{PL}$, the cross section of the QBHs production takes a form

$$\sigma = \frac{1}{16\pi}\frac{s}{\overline{M}_{PL}^4}\Theta(\sqrt{s}-\overline{M}_{PL}) \tag{1.3}$$

where we have assumed that the threshold mass for QBHs is identified with the Planck mass. Note that the QBHs described here are assumed to have a continuous mass spectrum despite some indications that their mass spectrum could be discrete [28]. Since we are considering a continuous mass spectrum we have to assume that quantum black hole couplings to long wavelength and highly off-shell perturbative modes are suppressed [11]. Otherwise their contribution to low energy observables such as K_L decays would have been noticed a long time ago. Note that there are no such constraints if the mass spectrum of QBHs is indeed discrete [29].

We shall first reconsider the production of spinless QBHs in the collisions of two fermions (quarks for example with the appropriate colour factor). We start with the Lagrangian

$$L_{\text{fermion+fermion}} = \frac{c}{\overline{M}_{PL}^2}\partial_\mu\partial^\mu\phi\bar{\psi}_1\psi_2 + h.c. \tag{1.4}$$

where c is the (non-local) parameter we will use to match the semiclassical cross section, $\overline{M}_{PL}$ is the reduced Planck mass, ϕ is a scalar field representing the quantum black hole, and ψ_i is a fermion field. The cross section for ϕ production is:

$$\sigma(2\psi\to\phi) = \frac{\pi}{s}\,|A|^2\,\delta(s-M_{BH}^2) \tag{1.5}$$

where M_{BH} is the mass of the black hole, $s=(p_1+p_2)^2$ and p_1,p_2 are the four-momenta of ψ_1 ψ_2. We find

$$|A|^2 = s^2\frac{c^2}{\overline{M}_{PL}^4}[s-(m_1+m_2)^2] \tag{1.6}$$

where m_1 and m_2 are the masses of the fermions ψ_1 and ψ_2. We now compare this cross section with the geometrical cross section. If we use the representation for the delta-function written in the form of the Poisson kernel,

$$\delta(s-M_{BH}^2) = \frac{\Gamma M_{BH}}{\pi[(s-M_{BH}^2)^2+\Gamma^2 M_{BH}^2]} \tag{1.7}$$

where Γ is the decay width of ϕ, we find:

$$c^2 = \frac{9}{4}\frac{4s^{\frac{3}{2}}-8sM_{BH}+4\sqrt{s}M_{BH}^2+\sqrt{s}\Gamma^2}{\Gamma\pi[s-(m_1+m_2)^2]} \tag{1.8}$$

Finally Γ can be calculated using the Lagrangian (1.4) as:

$$\Gamma = \frac{c^2}{8\pi}\frac{M_{BH}\sqrt{(M_{BH}^2-(m_1+m_2)^2)(M_{BH}^2-(m_1-m_2)^2)}}{\overline{M}_{PL}^4} \tag{1.9}$$

We can thus find an expression for our non-local parameter c by inserting Γ into the expression for c (1.8). In the case $m_1 = m_2 = 0$, one has a remarkably simple expression:

$$c^2 = \frac{8\pi \overline{M}_{PL}^4 (s - M_{BH}^2)}{M_{BH}^3 \sqrt{128\pi^2 \overline{M}_{PL}^4 s - M_{BH}^6}} \tag{1.10}$$

One can see that non-local behaviour of the c-coupling is quite non-trivial — it actually compensates the Breit-Wigner behaviour of the squared matrix element which would appear in case of constant c and leads to the expected s-dependence of the cross section from eq. (1.3). It is important to realize that QBHs do not appear as resonances since their parton level cross section is extrapolated from the semi-classical cross section as a function of s. With this in mind, we have also found an alternative approach to the construction of the QBH Lagrangian. If we recall that the Lagrangian for the four-fermion interactions

$$\mathcal{L}_{\text{cont}} = \frac{g_c}{\Lambda^2} \bar{\psi}_i \psi_i \bar{\psi}_j \psi_j \tag{1.11}$$

provides the squared matrix element for $\bar{\psi}_i \psi_i \to \bar{\psi}_j \psi_j$ scattering,

$$|M|^2 = \frac{g_c^2}{\Lambda^4} \tag{1.12}$$

and the respective total $\bar{\psi}_i \psi_i \to \bar{\psi}_j \psi_j$ cross section (neglecting the fermion masses)

$$\sigma = \frac{1}{16\pi s} |M|^2 = \frac{g_c^2}{16\pi} \frac{s}{\Lambda^4}, \tag{1.13}$$

then after comparison with eq. (1.3), we can immediately see that eq. (1.3) can be reproduced by 4-fermion interactions with $g_c = 1$ and $\Lambda = \overline{M}_{PL}$. Because of strong gravitational interactions at the scale M_{PL} , defined by taking the coupling $g_c = 1$, the production cross section for QBHs is at least as high as that for new KK-modes produced by the strong interactions. This makes QBHs one of the best objects to look for as the first effects from strong quantum gravity at the LHC.

In case of different fermion species involved in $2 \to 2$ process of the QBH production and decay, g_c will include the respective number of degrees of freedom to correctly reproduce the QBH branching fractions. In the scenario under study we consider the case of spin-0 neutral QBH production which preserves $SU(3) \times SU(2) \times U(1)$ gauge invariance but does not conserve flavour. We wish to emphasise that we are here only considering colourless QBHs which explains why our branching ratios are different from those of [4] (see also [30]). We have found that the most elegant and practical way to express these contact interactions is to use the auxiliary, non propagating scalar field, X which enters the following Lagrangian

$$\mathcal{L}_{\text{cont}}^X = g_c \left(\sum_{\text{leptons}} \bar{\psi}_i^\ell \psi_j^\ell X + \sum_{\text{quarks}} \bar{\psi}_i^q \psi_j^q X \right), \tag{1.14}$$

where i, j are lepton and quark flavour indices, propagator of "contact" X field is $\frac{i}{M_{PL}^2}$, $g_c = (n_l + 3n_q)^{-1/4}$ is the normalisation factor accounting number of charged lepton, $n_l = 9$

and quark, $n_q = 18$ combinations, including the quark colour factor. This Lagrangian exactly reproduces the cross section of the spinless neutral QBH production and decay in the $2 \to 2$ fermion process as a function of s at the parton level (up to the multiplicative trivial form-factor $FF = \Theta(\sqrt{s} - \overline{M}_{PL})$).

Our results could be generalised easily to the case of initial state particles with different spins and colours for which the approach of the contact interactions also works successfully as one can check using dimensional analysis approach.

The result can be also generalised to the case of higher dimensional QBHs for which the Schwarzschild radius is given by (see e.g. [7])

$$r_s(s, n, \overline{M}_{PL}) = k(n)\overline{M}_{PL}^{-1}(\sqrt{s}/\overline{M}_{PL})^{1/(1+n)} \tag{1.15}$$

where n is the number of extra-dimensions, $\overline{M}_{PL}$ the 4+n reduced Planck mass and $k(n)$ reads

$$k(n) = \left(2^n \sqrt{\pi}^{(n-3)} \frac{\Gamma((3+n)/2)}{2+n}\right)^{1/(1+n)}. \tag{1.16}$$

The respective form factors for the case of n-dimensions which should be introduced for the parton-level cross section to reproduce the correct cross section from the Lagrangian with contact interactions (1.14) is

$$FF = (4\pi k(n))^2 \left(\frac{\overline{M}_{PL}}{\sqrt{s}}\right)^{\frac{2n}{1+n}} \Theta(\sqrt{s} - \overline{M}_{PL}). \tag{1.17}$$

Here the case $n = 0$ corresponds to 4-dimensional models with low scale quantum gravity [4–6], $n = 1$ to Randall Sundrum [3] brane world model[1] and $n \geq 2$ to ADD model [1, 2]. Note that there are astrophysical constraints on $n = 2, 3, 4$ ADD which shift exclude a Planck mass in the few TeV region, it is however interesting to consider bounds from QBHs which are independent of those coming from Kaluza Klein modes which lead to the astrophysical constraints.

2 Phenomenology of the QBHs at the LHC

To study the phenomenology of the QBHs production we have implemented interactions given by eq. (1.14)–(1.17) into CalcHEP software package [31] as a QBH model which is publicly available at the High Energy Physics Model Database (HEPMDB) [32, 33] under the link http://hepmdb.soton.ac.uk/hepmdb:1113.0146. We also would like to note an important feature of CalcHEP which allows the implementation of non-trivial form factors at the user level which was one of the key points in the implementation of this model. We emphasise that the Lagrangian we are proposing to describe the interactions of QBHs with particles of the Standard Model should not be regarded as an effective theory in the usual sense, it is rather an effective manner to describe the interactions of these black holes with usual particles.

[1]Note that will treat the Randall Sundrum QBHs as ADD ones with $n = 1$. While the cross section for semi-classical black holes in the case of RS differs from that obtained using the Schwarzschild metric [20], this is an unnecessary refinement for QBHs whose quantum geometry is anyway very poorly understood.

	$\overline{M}_{PL}$ (TeV)	n=0	n=1	n=2	n=3	n=4	n=5	n=6
LHC@8TeV	1.0	32.3	782.	2760.	5730.	9370.	13500.	18100.
	2.0	0.235	6.60	24.5	51.8	85.7	124.	166.
	3.0	0.00388	0.116	0.439	0.939	1.56	2.28	3.06
LHC@13TeV	1.0	177.	373.	12800.	26000.	42200.	60500.	80400.
	2.0	3.11	79.7	286.	596.	980.	1420.	1890.
	3.0	0.161	4.48	16.5	34.8	57.4	83.5	112.

Table 1. The cross section for $pp \to QBH(0,0) \to e^-\mu^+(+e^+\mu^-)$ process at the LHC in fb for 8 TeV and 13 TeV centre-of-mass energy pp collisions for $\overline{M}_{PL}$=1,2,3 TeV and n=1-6.

This model is publicly available at HEPMDB which provides HEP community with a new QBH Monte-Carlo (MC) generator (QBH@HEPMDB), and is an alternative to existing BlackMax [10] and QBH [34] MC generators. We would like to stress that QBH@HEPMDB model is available for download and allows (at HEPMDB website or using CalcHEP locally) to evaluate cross sections and generate parton-level events in generic Les Houches Event (LHE) format [35] which can be *independently* used in subsequent analysis using various general purpose MC generators and detector simulation software. In this paper we present the first phenomenological application of the QBH@HEPMDB model with spin-0 neutral QBH [QBH(0,0)] to e^+e+ and $e\mu$ signature at the LHC@8TeV and LHC@13TeV. We produce the respective projections for the LHC to probe QBH parameter space. The model can be easily extended for QBHs with other charges and spins using the same approach as described above. In our calculations we have used CTEQ6L [36] parameterisation for the parton density functions (PDFs) while the QCD scale was fixed to $\overline{M}_{PL}$. The parameter space of the model under study is the reduced Planck mass, $\overline{M}_{PL}$, which sets the threshold for the QBH production as well the number of the extra-dimensions n.

We start by presenting the QBH production cross section in figure 1 where the cross section versus $\overline{M}_{PL}$ (upper row) and versus n (bottom row) is given for $pp \to QBH(0,0) \to e^-\mu^+(+e^+\mu^-)$ process at the LHC for 8 TeV (left) and 13 TeV (right) centre-of-mass energy pp collisions. The respective specific numbers for the cross section are given in table 1. Note that the cross section for $pp \to QBH(0,0) \to e^-e^+$ production is a factor of two smaller because of the respective QBH branching ratio. One can observe a big difference in cross sections between effective four-dimensional case ($n = 0$) and higher dimensional theories, for which the cross section of QBH production can be three orders of magnitude higher as, for example, for $n = 6$ case, when the cross section driven by the factor (1.17). The cross section dependence as a function of n is explicitly presented in the bottom row of figure 1 for three fixed values of $\overline{M}_{PL} = 1, 2, 3$ TeV. One can note that the steep cross section drop as a function of $\overline{M}_{PL}$ is defined by PDFs and reaches 0.1 fb around $\overline{M}_{PL} = 2$ TeV for $n = 0$ and around $\overline{M}_{PL} = 4$ TeV for $n = 6$ at the LHC@8TeV. At the LHC@13TeV the cross section reaches 0.1 fb around $\overline{M}_{PL} = 3$ TeV for $n = 0$ and around $\overline{M}_{PL} = 6$ TeV for $n = 6$. Let us note that 0.1 fb cross section level is the typical sensitivity which is expected

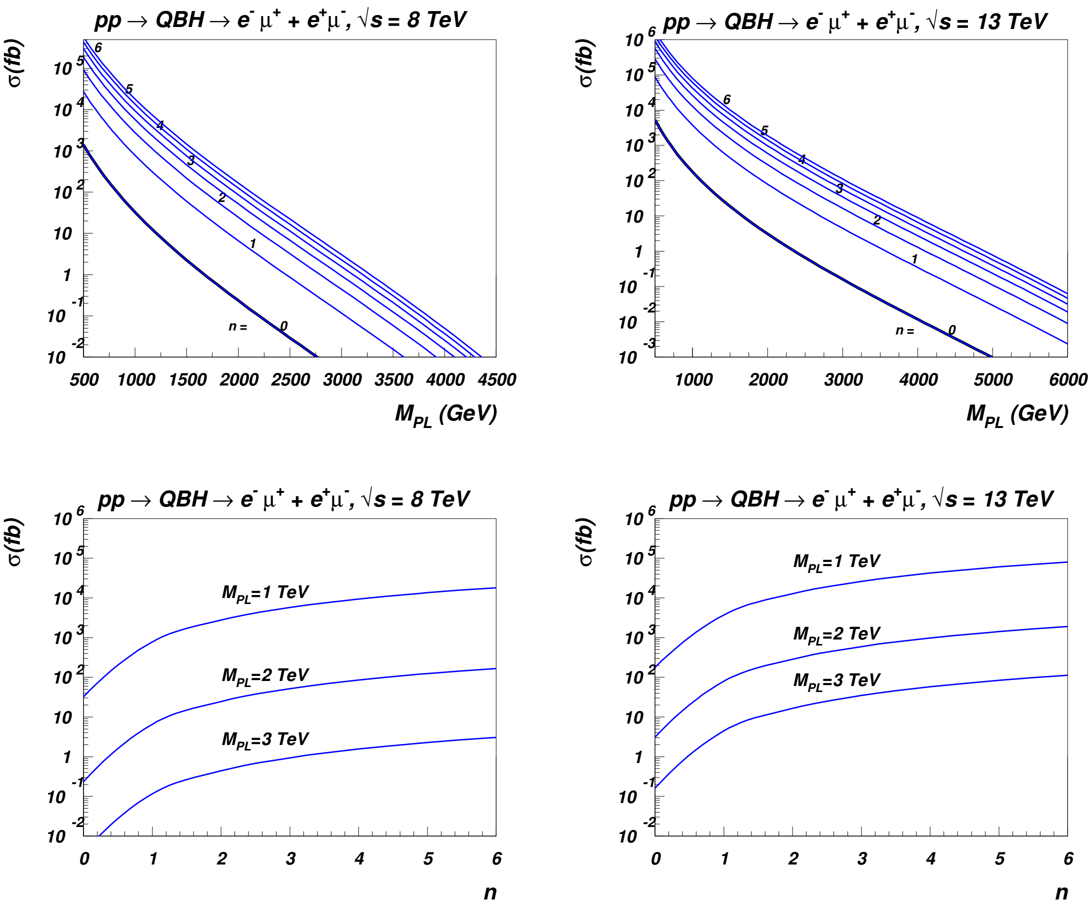

Figure 1. The cross section of $pp \to QBH(0,0) \to e^-\mu^+(+e^+\mu^-)$ process at the LHC for 8 TeV (left) and 13 TeV (right) centre-of-mass energy pp collisions. Upper row: cross section versus $\overline{M}_{PL}$, bottom row: cross section versus n.

at 20 fb^{-1} at LHC@8TeV or 30 fb^{-1} at LHC@13TeV (first year run) luminocities providing respectively few events which under assumption of the negligible background allows to establish exclusion at the 95% CL. It is worth discussing the *shape* of the kinematical distributions from QBH(0,0) decay products. In figure 2 we present $e\mu$ invariant mass distribution for different n for LHC for 8 TeV (left) and 13 TeV (right) and $\overline{M}_{PL} = 1$(left) and 2 TeV (right). Results are presented for the same normalisation to compare the shapes of the distributions for different n. The signal shape exhibits a threshold production nature and driven primarily by PDFs, whose fall is much steeper with the energy than the increase of the parton-level cross section. Therefore the mass of the QBH is primarily distributed around the M_{PL}. It is qualitatively different from a Breit-Wigner shape of resonances, e.g. Z' bosons, appearing in various BSM models. One can observe the shape difference between different extra-dimensional models and the effective four-dimensional theory. Moreover, the more phase space is available, the bigger difference in the high invariant mass tail which drops faster for larger number of extra dimensions. This is actually what one can expect

JHEP08(2015)139

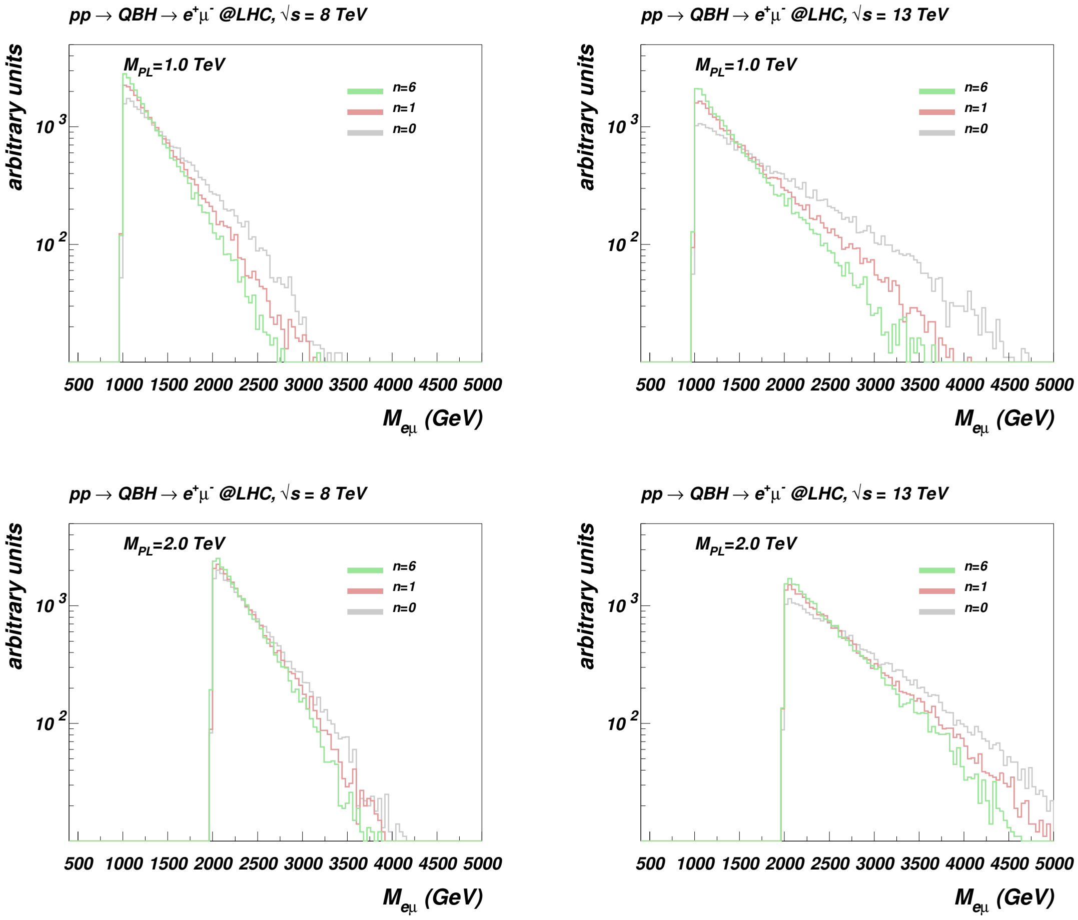

Figure 2. Invariant mass of $e\mu$ distribution for different n for LHC for 8 TeV (left) and 13 TeV (right) and $\overline{M}_{PL} = 1$(left) and 2 TeV (right). Results are presented with the same normalisation.

recalling the energy dependent nature of the form-factor given by eq. (1.17). So, $n = 0$[2] distributions has the slowest $M_{e\mu}$ dependence which sharpens with the increase of n driven by eq. (1.17). One can see that in the large n limit the parton level asymptotically becomes less and less s dependent, so $M_{e\mu}$ distributions become similar and are defined by rapidly falling PDFs. One should also note that all $M_{e\mu}$ distributions, exhibit a clear step at the QBH production threshold and are qualitatively different from the resonant Breit-Wigner shape. Therefore in our analysis of the LHC sensitivity to the QBH parameter space, we set a lower $M_{e\mu}$ cut rather than a mass-window cut.

Lets turn now to p_T^ℓ distribution presented in figure 3. One can see that the difference between transverse momentum distributions is clearly connected with s dependence of eq. (1.17) and eventually correlated with differences in $M_{e\mu}$ distributions. At the same

[2]Note that the limit for $n = 0$ obtained here does apply to the specific models described in [4–6] since these models have large hidden sectors and neutral QBHs would decay massively in the particles of the hidden sector. However, charged black holes, which are not considered here, would decay into standard model particles.

JHEP08(2015)139

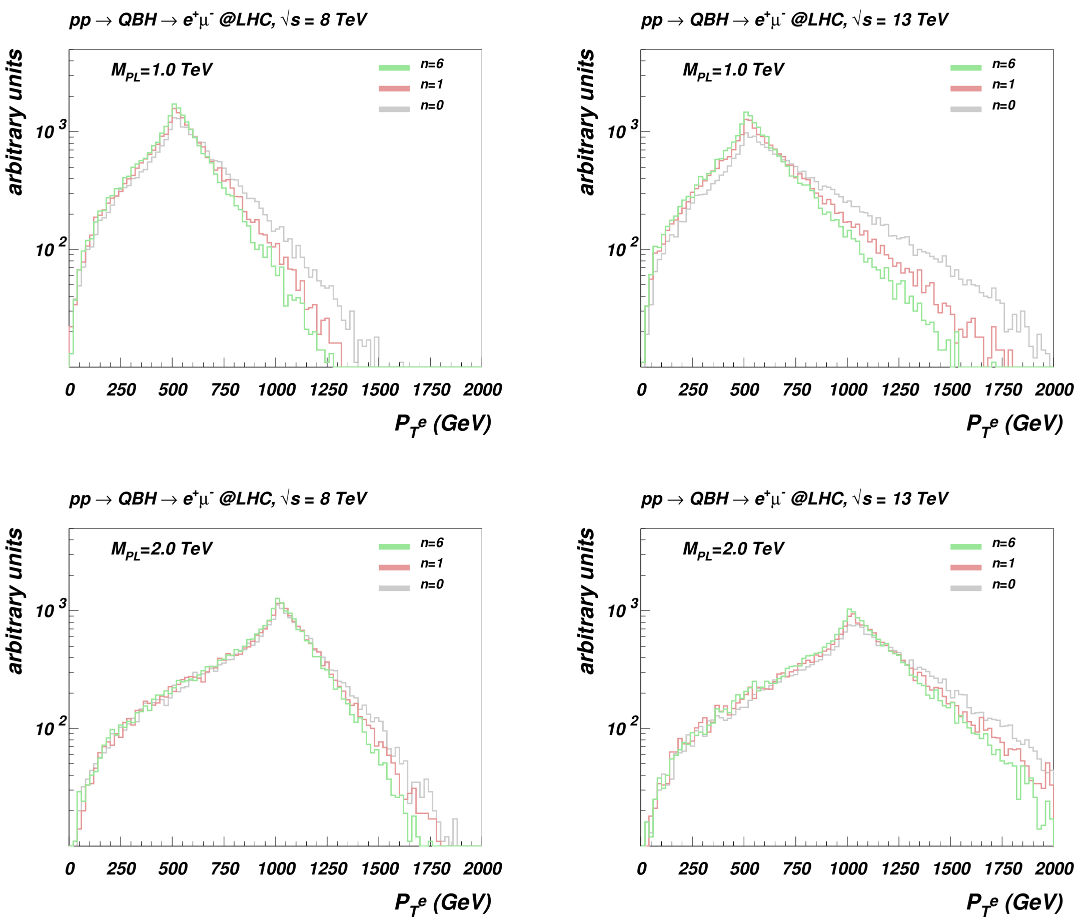

Figure 3. p_T^ℓ distribution for different n for LHC for 8 TeV (left) and 13 TeV (right) and $\overline{M}_{PL} =$ 1(left) and 2 TeV (right). Results are presented for the same normalisation.

time it is worth noting that the difference in the high energy tail distribution will not visibly affect acceptance/selection cuts as we discuss below. Finally lets take a look at the pseudorapidity distributions in bottom left frame of figure 4 which demonstrate that η_ℓ distributions are very similar for the scenarios with different n. Looking at figure 2–4 one can conclude that in spite of the differences for certain kinematical distributions for different n for high values of $M_{\mu e}$ and $P_T^{e,\mu}$, one can expect a very similar acceptance efficiency for these models, since all of them provide high P_T leptons (with P_T far above the acceptance cuts) with a very similar rapidity distributions.

We have also performed signal vs background analysis for the QBH(0,0) production at the LHC decaying into e^+e^- and $e\mu$ final states. The main backgrounds for the e^+e^- signature are $pp \to e^+e^-$ Drell-Yan (DY) process, as well as $\bar{t}t$ and W^+W^- pair production. The rate of these backgrounds together with the signal rate for $\overline{M}_{PL} = 0.5$, 1 and 2 TeV is presented in figure 5(left) for $M_{e^+e^-}$ invariant mass distribution. The QBH signal is shown for $n = 0$ case. One can see that the dominant DY background is below the signal, but it is not negligible for M_{PL} around 0.5-1 TeV. At the same time DY background is

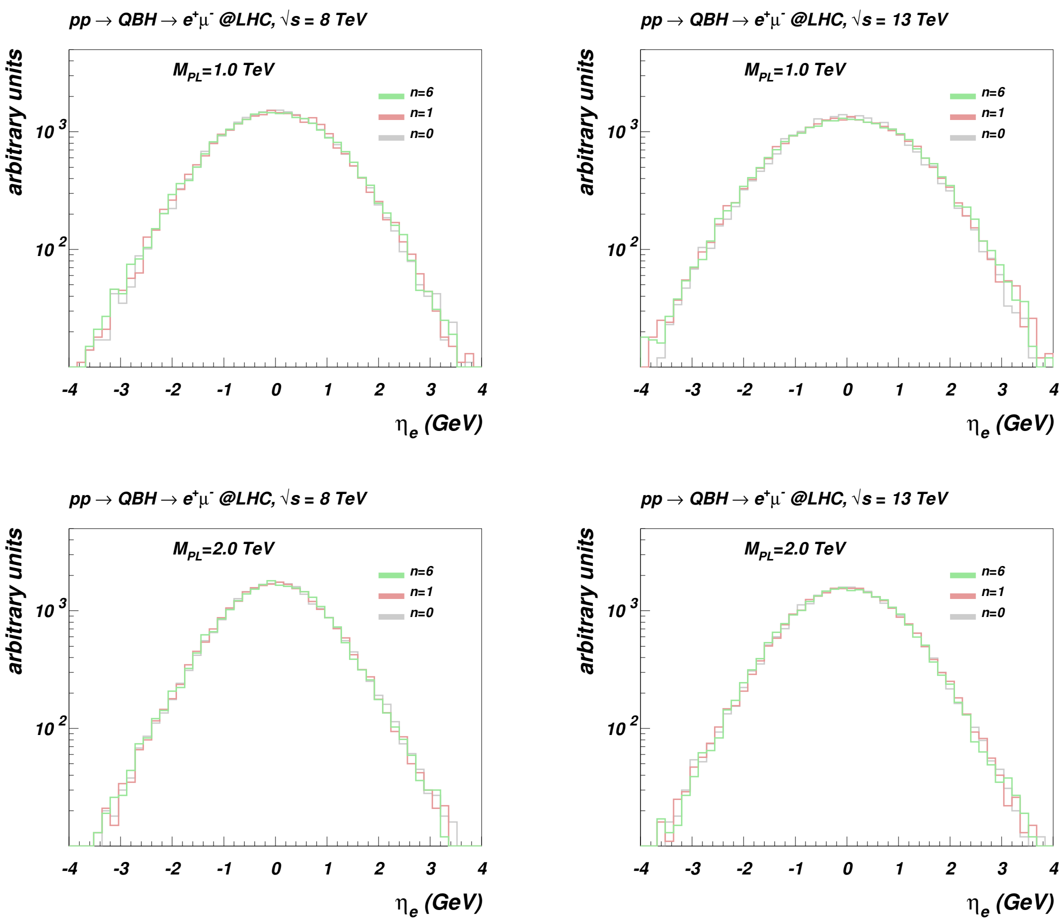

Figure 4. Pseudorapidity of lepton distribution for different n for LHC for 8 TeV (left) and 13 TeV (right) and $\overline{M}_{PL} = 1$(left) and 2 TeV (right). Results are presented for the same normalisation.

absent in case of $e\mu$ signature, as shown in figure 5(right). One can also see that in case of this signature $\bar{t}t$ and W^+W^- backgrounds are negligible, so LHC potential to probe this signature purely depends on the signal rate which is defined by $\overline{M}_{PL}$ and n parameters. Analogous distributions are presented in figure 6 for LHC@13 TeV exhibiting qualitatively the same pattern for signal and backgrounds for the e^+e^- and $e\mu$ signatures under study.

At the final step we estimate discovery and exclusion sensitivity of the LHC@8 and LHC@13 TeV to di-lepton signature from the QBH production under study.

In our analysis though we restrict ourselves to the study at parton-level and do take into account realistic electromagnetic energy resolution, using a value of $0.15/\sqrt{E(\text{GeV})}$, which is typical for the ATLAS and CMS detectors and require $|\eta_{\mu,e}| < 2.5$ and $p_T^{e,\mu}$ with respect to the acceptance cuts. We also suggest the simple analysis cut to be $M_{e\mu}(M_{ee}) > 1.1 \times \overline{M}_{PL}$, noting that the acceptance efficiency will be very similar for different n models. In figure 7 we present the signal significance for QBH signatures under study at the LHC. For both criteria, exclusion and discovery, we use the following formula for statistical signal

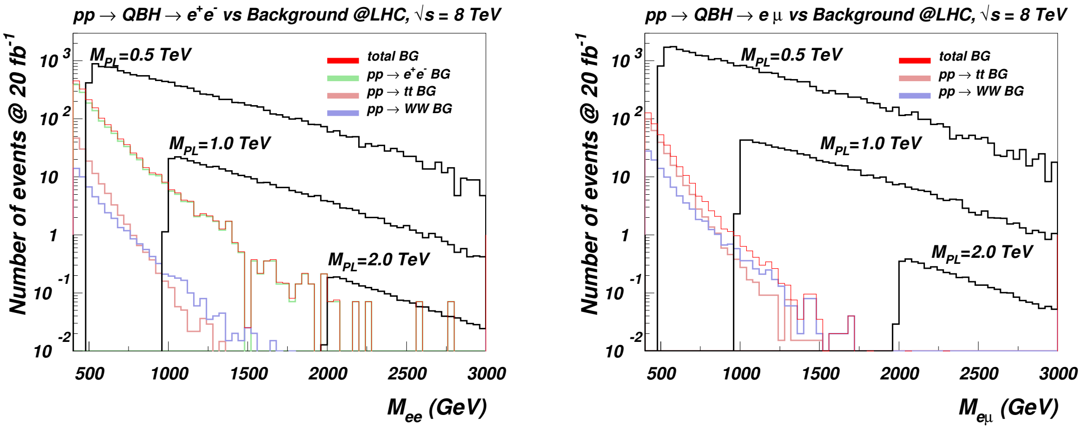

Figure 5. Invariant mass distributions for e^+e^- (left) and $e\mu$ (right) QBH signatures ($n = 0$ case) and the respective backgrounds for LHC@8TeV.

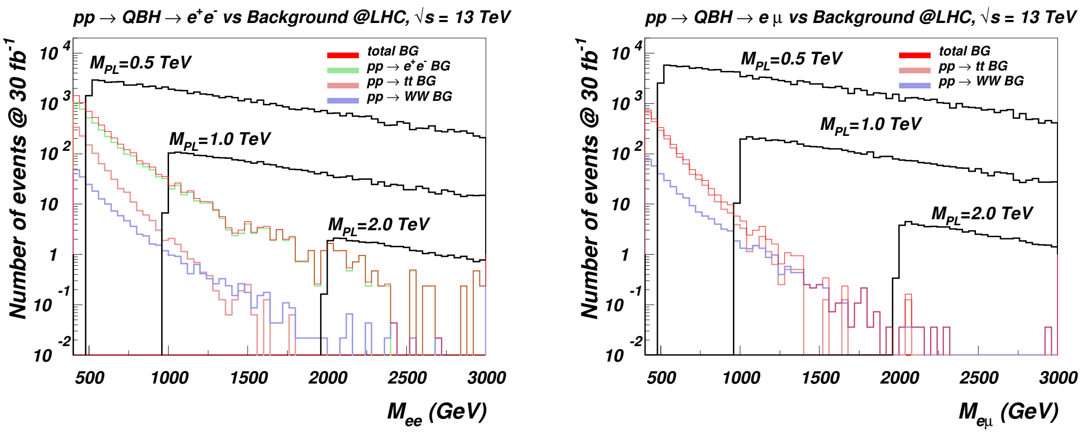

Figure 6. Invariant mass distributions for e^+e^- (left) and $e\mu$ (right) QBH signatures ($n = 0$ case) and the respective backgrounds for LHC@13TeV.

significance α as [37]

$$\alpha = 2(\sqrt{N_S + N_B} - \sqrt{N_B}) \tag{2.1}$$

and require $\alpha \geq 2$ for exclusion region and $\alpha \geq 5$ for the discovery region. The $N_{S(B)} = \sigma_{S(B)}\mathcal{L}$ denotes the number of signal (background) events for an integrated luminosity $\mathcal{L}$. The figure presents results for LHC@8 ($20\,\text{fb}^{-1}$) and 13 TeV ($30\,\text{fb}^{-1}$) for $n = 0$ and 6 as two extreme cases for the range of n under study. The

The respective $\overline{M}_{PL}$ exclusion and discovery limits for LHC@8 and 13 TeV for $n = 0$ and $n = 6$ scenarios are presented in table 2. One can see that for $n = 0$ the LHC@8TeV the limit on $\overline{M}_{PL}$ @95% CL is only about 1.92 TeV for e^+e^- signature and 2.24 TeV for $e\mu$ one, while the respective discovery numbers are 1.55 and 1.81 TeV respectively. The LHC@13TeV in the first year will be able to improve limits and cover $\overline{M}_{PL}$ @95% CL

JHEP08(2015)139

		LHC@8TeV		LHC@13TeV	
CL	n	e^+e^-	$e\mu$	e^+e^-	$e\mu$
95%CL	0	1920 GeV	2240 GeV	3360 GeV	3780 GeV
5σ	0	1550 GeV	1810 GeV	2790 GeV	3180 GeV
95%CL	6	3540 GeV	3680 GeV	5510 GeV	5750 GeV
5σ	6	3140 GeV	3300 GeV	4850 GeV	5100 GeV

Table 2. $\overline{M}_{PL}$ exclusion and discovery limits for LHC@8 and 13 TeV for $n = 0$ and $n = 6$ scenarios.

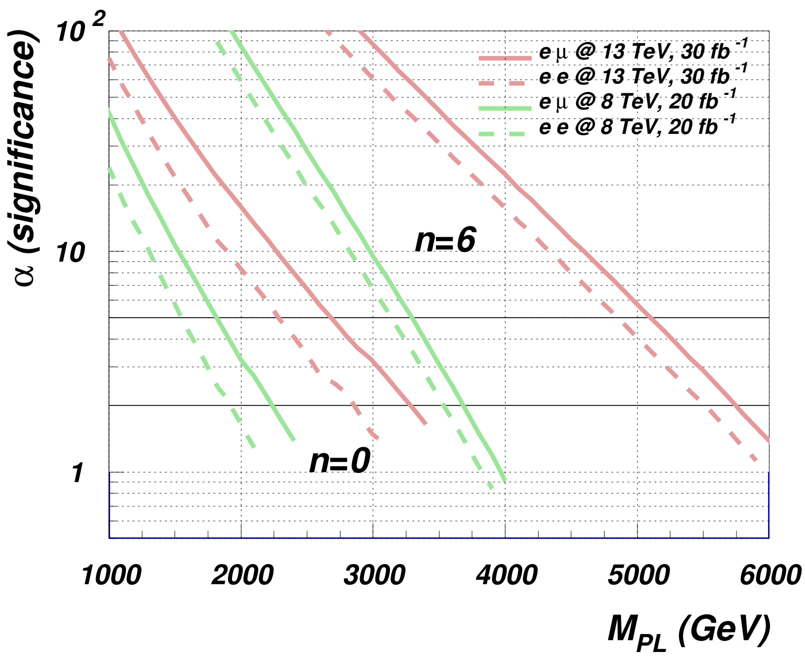

Figure 7. Signal significance for QBH e^+e^- and $e\mu$ signatures as a function of $\overline{M}_{PL}$ for $n = 0$ and 6 at the LHC@8 and 13 TeV.

up to 3.36 TeV with e^+e^- signature and up to 3.78 TeV with $e\mu$, and discover QBH with $\overline{M}_{PL}$ up to 2.79 and 3.18 TeV respectively. At the same time the for $n = 6$ for which the QBH production cross section is about 3 orders of magnitude higher, the LHC reach is much more impressive. For example, with $e\mu$ signature LHC@8 will be able to exclude $\overline{M}_{PL} < 3.68$ TeV @95% CL or discover QBH with $\overline{M}_{PL} < 3.30$ TeV. Analogous numbers for LHC@13TeV are even more exciting — it would be able to probe $\overline{M}_{PL} < 5.75$ TeV or discover the $e\mu$ signal for $\overline{M}_{PL} < 5.10$ TeV. In is worth noting that though our analysis reproduces quite well recent ATLAS results on QBH search at LHC@8TeV [38], which stated the 3.65 TeV limit for $n = 6$ case for $e^+e^- + \mu^+\mu^-$ signatures. Since the signal cross section for this signature equal to the cross section for the $e\mu$ signal while background is negligible, the limits are expected to be the same for both cases. The respective limit from our study is 3.67 TeV which is in a very good agreement with the above on from ATLAS. We should also mention that the signal cross section, quoted by [38] for $n = 6$ case agrees within 10% with the cross section we found in our paper. Therefore we can also conclude about the successful validation of our generator and analysis for the LHC@8TeV.

3 Conclusions

QBHs production at the scale M_{PL} provides one of the best opportunities to look for the first possible effect from strong quantum gravity at the LHC. We discuss a field theoretical framework to describe the interactions of non-thermal QBHs with particles of the Standard Model and propose a non-local Lagrangian to describe the production of these QBHs which is designed to reproduce the geometrical cross section πr_s^2 for black hole production.

We have implemented this model into CalcHEP and it is publicly available at the High Energy Model Database for simulation of QBH events at the LHC and future colliders. QBH@HEPMDB is the CalcHEP's model and the MC generator at the same time. It is an effective independent tool for QBH phenomenological and experimental explorations. One should stress that the QBH@HEPMDB MC generator is based on a simple and transparent model, which can be easily updated to include QBH of higher spins. This makes our MC generator very flexible and easily extendable. This can simply be done by extending the table of Feynman Rules and particles of the model thereby avoiding any additional programming. Detailed comparison of QBH@HEPMDB with analogous tools on the market requires dedicated work which we plan to perform in the nearest future.

In this paper we present the first phenomenological application of the QBH@HEPMDB model with spin-0 neutral QBH giving rise the e^+e^- and $e\mu$ signatures at the LHC@8TeV and LHC@13TeV and produce the first respective projections in terms of limits on the reduced Planck mass, $\overline{M}_{PL}$ and the number of the extra-dimensions n. In particular we found that among two signatures, $e\mu$ one provides the best LHC reach since it is free of DY background. We have successfully validated our generator and exclusion limits against recent ATLAS results for $n = 6$ case. We found that with $e\mu$ signature, for number of extra-dimensions, n, in the range of 0-6, the LHC@8 will be able to probe the respective range of 2.2-3.7 TeV of the reduced Planck Mass $\overline{M}_{PL}$. We have also produced new projections for LHC@13 and found that even in the first year of operation with $30 fb^{-1}$ the range 3.8-5.8 TeV of $\overline{M}_{PL}$ at 95%CL can be probed. The respective discovery range of LHC@13 is 3.2-5.1 TeV for $\overline{M}_{PL}$.

Acknowledgments

We are grateful to Tim Morris, Alexander Pukhov, Claire Shepherd-Themistocleous, Emmanuel Olaiya, Andreas Gueth, Thomas Reis and Ilya Shapiro for stimulating discussions. This work is supported in part by the European Cooperation in Science and Technology (COST) action MP0905 "Black Holes in a Violent Universe" and by the Science and Technology Facilities Council, grants number ST/L000504/1 and ST/L000296/1.

JHEP08(2015)139

References

[1] N. Arkani-Hamed, S. Dimopoulos and G.R. Dvali, *The hierarchy problem and new dimensions at a millimeter*, Phys. Lett. **B 429** (1998) 263 [hep-ph/9803315] [INSPIRE].

[2] I. Antoniadis, N. Arkani-Hamed, S. Dimopoulos and G.R. Dvali, *New dimensions at a millimeter to a Fermi and superstrings at a TeV*, Phys. Lett. **B 436** (1998) 257 [hep-ph/9804398] [INSPIRE].

[3] L. Randall and R. Sundrum, *A large mass hierarchy from a small extra dimension*, Phys. Rev. Lett. **83** (1999) 3370 [hep-ph/9905221] [INSPIRE].

[4] X. Calmet, S.D.H. Hsu and D. Reeb, *Quantum gravity at a TeV and the renormalization of Newton's constant*, Phys. Rev. **D 77** (2008) 125015 [arXiv:0803.1836] [INSPIRE].

[5] X. Calmet, *A review of quantum gravity at the Large Hadron Collider*, Mod. Phys. Lett. **A 25** (2010) 1553 [arXiv:1005.1805] [INSPIRE].

[6] X. Calmet, *The lightest of black holes*, Mod. Phys. Lett. **A 29** (2014) 1450204 [arXiv:1410.2807] [INSPIRE].

[7] S. Dimopoulos and G.L. Landsberg, *Black holes at the LHC*, Phys. Rev. Lett. **87** (2001) 161602 [hep-ph/0106295] [INSPIRE].

[8] T. Banks and W. Fischler, *A model for high-energy scattering in quantum gravity*, hep-th/9906038 [INSPIRE].

[9] S.B. Giddings and S.D. Thomas, *High-energy colliders as black hole factories: the end of short distance physics*, Phys. Rev. **D 65** (2002) 056010 [hep-ph/0106219] [INSPIRE].

[10] D.-C. Dai, G. Starkman, D. Stojkovic, C. Issever, E. Rizvi and J. Tseng, *BlackMax: a black-hole event generator with rotation, recoil, split branes and brane tension*, Phys. Rev. **D 77** (2008) 076007 [arXiv:0711.3012] [INSPIRE].

[11] X. Calmet, W. Gong and S.D.H. Hsu, *Colorful quantum black holes at the LHC*, Phys. Lett. **B 668** (2008) 20 [arXiv:0806.4605] [INSPIRE].

[12] J.L. Feng and A.D. Shapere, *Black hole production by cosmic rays*, Phys. Rev. Lett. **88** (2002) 021303 [hep-ph/0109106] [INSPIRE].

[13] L.A. Anchordoqui, J.L. Feng, H. Goldberg and A.D. Shapere, *Inelastic black hole production and large extra dimensions*, Phys. Lett. **B 594** (2004) 363 [hep-ph/0311365] [INSPIRE].

[14] L.A. Anchordoqui, J.L. Feng, H. Goldberg and A.D. Shapere, *Black holes from cosmic rays: probes of extra dimensions and new limits on TeV scale gravity*, Phys. Rev. **D 65** (2002) 124027 [hep-ph/0112247] [INSPIRE].

[15] L.A. Anchordoqui, J.L. Feng, H. Goldberg and A.D. Shapere, *Updated limits on TeV scale gravity from absence of neutrino cosmic ray showers mediated by black holes*, Phys. Rev. **D 68** (2003) 104025 [hep-ph/0307228] [INSPIRE].

[16] X. Calmet and M. Feliciangeli, *Bound on four-dimensional Planck mass*, Phys. Rev. **D 78** (2008) 067702 [arXiv:0806.4304] [INSPIRE].

[17] X. Calmet, L.I. Caramete and O. Micu, *Quantum black holes from cosmic rays*, *JHEP* **11** (2012) 104 [arXiv:1204.2520] [INSPIRE].

[18] N. Arsene, X. Calmet, L.I. Caramete and O. Micu, *Back-to-back black holes decay signature at neutrino observatories*, *Astropart. Phys.* **54** (2014) 132 [arXiv:1303.4603] [INSPIRE].

[19] X. Calmet, B. Carr and E. Winstanley, *Quantum black holes*, Springer Briefs in Physics, Spinger, Germany (2013) [ISBN-10:3642389384] [ISBN-13:978-3642389382] [INSPIRE].

[20] P. Meade and L. Randall, *Black holes and quantum gravity at the LHC*, *JHEP* **05** (2008) 003 [arXiv:0708.3017] [INSPIRE].

[21] D.M. Eardley and S.B. Giddings, *Classical black hole production in high-energy collisions*, *Phys. Rev.* **D 66** (2002) 044011 [gr-qc/0201034] [INSPIRE].

[22] P.D. D'Eath and P.N. Payne, *Gravitational radiation in high speed black hole collisions.* 1. *Perturbation treatment of the axisymmetric speed of light collision*, *Phys. Rev.* **D 46** (1992) 658 [INSPIRE].

[23] P.D. D'Eath and P.N. Payne, *Gravitational radiation in high speed black hole collisions.* 2. *Reduction to two independent variables and calculation of the second order news function*, *Phys. Rev.* **D 46** (1992) 675 [INSPIRE].

[24] P.D. D'Eath and P.N. Payne, *Gravitational radiation in high speed black hole collisions.* 3. *Results and conclusions*, *Phys. Rev.* **D 46** (1992) 694 [INSPIRE].

[25] S.D.H. Hsu, *Quantum production of black holes*, *Phys. Lett.* **B 555** (2003) 92 [hep-ph/0203154] [INSPIRE].

[26] X. Calmet, D. Fragkakis and N. Gausmann, *The flavor of quantum gravity*, *Eur. Phys. J.* **C 71** (2011) 1781 [arXiv:1105.1779] [INSPIRE].

[27] X. Calmet, D. Fragkakis and N. Gausmann, *Non thermal small black holes*, in *Black holes: evolution, theory and thermodynamics*, chapter 8, A.J. Bauer and D.G. Eiffel eds., Nova Publishers, New York U.S.A. (2012) [arXiv:1201.4463] [INSPIRE].

[28] X. Calmet and N. Gausmann, *Non-thermal quantum black holes with quantized masses*, *Int. J. Mod. Phys.* **A 28** (2013) 1350045 [arXiv:1209.4618] [INSPIRE].

[29] X. Calmet, *Fundamental physics with black holes*, in *Quantum aspects of black holes*, chapter 1, X. Calmet ed., Springer, Germany (2015) [*Fundam. Theor. Phys.* **178** (2015) 1] [ISBN:978-3-319-10851-3] [INSPIRE].

[30] D.M. Gingrich, *Quantum black holes with charge, colour and spin at the LHC*, *J. Phys.* **G 37** (2010) 105008 [arXiv:0912.0826] [INSPIRE].

[31] A. Belyaev, N.D. Christensen and A. Pukhov, *CalcHEP* 3.4 *for collider physics within and beyond the standard model*, *Comput. Phys. Commun.* **184** (2013) 1729 [arXiv:1207.6082] [INSPIRE].

[32] M. Bondarenko et al., *High energy physics model database: towards decoding of the underlying theory*, in *Les Houches* 2011*: physics at TeV colliders new physics working group report*, arXiv:1203.1488 [INSPIRE].

[33] *HEPMDB: High Energy Physics Model Data Base webpage*, https://hepmdb.soton.ac.uk.

[34] D.M. Gingrich, *Monte Carlo event generator for black hole production and decay in proton-proton collisions*, *Comput. Phys. Commun.* **181** (2010) 1917 [arXiv:0911.5370] [INSPIRE].

JHEP08(2015)139

[35] J. Alwall et al., *A standard format for Les Houches event files*, *Comput. Phys. Commun.* **176** (2007) 300 [hep-ph/0609017] [INSPIRE].

[36] J. Pumplin, D.R. Stump, J. Huston, H.L. Lai, P.M. Nadolsky and W.K. Tung, *New generation of parton distributions with uncertainties from global QCD analysis*, *JHEP* **07** (2002) 012 [hep-ph/0201195] [INSPIRE].

[37] S.I. Bityukov and N.V. Krasnikov, *On the observability of a signal above background*, *Nucl. Instrum. Meth.* **A 452** (2000) 518 [INSPIRE].

[38] ATLAS collaboration, *Search for high-mass dilepton resonances in pp collisions at* $\sqrt{s} = 8$ *TeV with the ATLAS detector*, *Phys. Rev.* **D 90** (2014) 052005 [arXiv:1405.4123] [INSPIRE].

JHEP08(2015)139